Impact of an Updated Carbon Bond Mechanism on Predictions from the CMAQ Modeling System: Preliminary Assessment

GOLAM SARWAR AND DEBORAH LUECKEN

Atmospheric Modeling Division, National Exposure Research Laboratory, U.S. Environmental Protection Agency, Research Triangle Park, North Carolina

GREG YARWOOD

ENVIRON International Corporation, Novato, California

GARY Z. WHITTEN

Smog Reyes, Point Reyes Station, California

WILLIAM P. L. CARTER

CE-CERT, University of California, Riverside, California

(Manuscript received 13 January 2006, in final form 28 March 2007)

ABSTRACT

An updated and expanded version of the Carbon Bond mechanism (CB05) has been incorporated into the Community Multiscale Air Quality (CMAQ) modeling system to more accurately simulate wintertime, pristine, and high-altitude situations. The CB05 mechanism has nearly 2 times the number of reactions relative to the previous version of the Carbon Bond mechanism (CB-IV). While the expansions do provide more detailed treatment of urban areas, most of the new reactions involve biogenics, toxics, and species potentially important to particulate formation and acid deposition. Model simulations were performed using the CB05 and the CB-IV mechanisms for the winter and summer of 2001. For winter with the CB05 mechanism, ozone, aerosol nitrate, and aerosol sulfate concentrations were within 1% of the results obtained with the CB-IV mechanism. Organic carbon concentrations were within 2% of the results obtained with the CB-IV mechanism. However, formaldehyde and hydrogen peroxide concentrations were lower by 25% and 32%, respectively, during winter with the CB05 mechanism. For the summer, ozone concentrations increased by 8% with the CB05 mechanism relative to the CB-IV mechanism. The aerosol sulfate, aerosol nitrate, and organic carbon concentrations with the CB05 mechanism decreased by 8%, 2%, and 10%, respectively. The formaldehyde and hydrogen peroxide concentrations with the CB05 mechanism were lower by 12% and 47%, respectively, during summer. Model performance with the CB05 mechanism improved at high-altitude conditions and in rural areas for ozone. Model performance also improved for organic carbon with the CB05 mechanism.

1. Introduction

Air quality models (AQMs) that can realistically describe the formation of ozone (O_3), air toxics, and other pollutants are needed by the U.S. Environmental Protection Agency (EPA), state, and local agencies to predict current and future concentrations of these pollutants and develop emissions control strategies to decrease their concentrations below harmful levels. A critical component of these models is the description of complex atmospheric photochemistry, namely the gas-phase chemical mechanism. The chemical mechanisms used in three-dimensional (3D) AQMs must strike a balance between complexity and computational efficiency. For a 3D Eulerian grid model, the computational efficiency of its chemical mechanism is of high

Corresponding author address: Golam Sarwar, Atmospheric Modeling Division, National Exposure Research Laboratory, U.S. Environmental Protection Agency, Research Triangle Park, NC 27711.
E-mail: sarwar.golam@epa.gov

DOI: 10.1175/2007JAMC1393.1

priority, whereas for box models or 3D models over small spatial scales and short time periods the chemical detail may be important. Several methods for developing chemical mechanisms, and addressing this balance, were reviewed by Dodge (2000).

The Carbon Bond lumped-structure approach was originally developed in the late 1970s (Whitten et al. 1980). The Carbon Bond IV (CB-IV) mechanism (Gery et al. 1989) is a widely used chemical mechanism in urban to regional air quality modeling systems for many years. Computational efficiency was a high priority during the development of the CB-IV mechanism, and although the resulting mechanism is highly condensed, it is among the fastest of the commonly used chemical mechanisms. At the time of its inception, this high degree of condensation was appropriate given the existing knowledge of atmospheric chemistry, and for the predominant uses of AQMs, primarily for urban simulations.

The CB-IV mechanism has had several updates since its initial release (Zaveri and Peters 1999; Adelman 1999), but none has had widespread use in air quality models. Building on these earlier modifications, as well as on advancements made in the Statewide Air Pollution Research Center (SAPRC-99) mechanism (Carter 2000), the CB-IV mechanism has recently been updated and named the CB05 mechanism to signify its development in 2005 (Yarwood et al. 2005). Because of the widespread use of Carbon Bond–type mechanisms in AQMs, we have implemented the CB05 mechanism into the EPA's Community Multiscale Air Quality (CMAQ) modeling system. Here we briefly describe the updated mechanism and present a preliminary evaluation of the effect of this mechanism on selected species under both winter and summer conditions.

2. Methodology

a. Model description

The EPA's CMAQ modeling system (version 4.5; Binkowski and Roselle 2003; Byun and Schere 2006) was used for this study. Model performance evaluations for this modeling system have been conducted by comparing model predictions to measured ambient pollutants obtained from several measurement networks (Appel et al. 2007). For this study, the horizontal domain of the model consisted of 148×112 grid cells with a 36-km grid spacing with 14 layers in the vertical direction. The CMAQ chemical transport model was configured to use the newly developed mass continuity scheme in version 4.5 to describe the advection processes, the multiscale method to describe the horizontal diffusion processes, the eddy diffusion method to describe the vertical diffusion processes, and the asymmetrical convective model for cloud processes. Aqueous chemistry, aerosol processes, and dry and wet deposition were also included, but the plume-in-grid treatment was not. The CMAQ modeling system currently provides three different gas-phase chemistry solvers: the Sparse-Matrix Vectorized Gear solver, the Rosenbrock solver, and the Euler Backward Iterative solver; the Rosenbrock solver was used in this study. The meteorological driver for the CMAQ modeling system was the fifth-generation Pennsylvania State University–National Center for Atmospheric Research Mesoscale Model (MM5, version 3.5; Grell et al. 1994). The meteorological data obtained from the MM5 system were processed using the Meteorology–Chemistry Interface Processor (MCIP, version 2.3; Byun and Schere 2006).

The predefined clean-air vertical profiles provided in the CMAQ modeling system were used. The model was spun up for 10 days to minimize the effect of initial conditions on model predictions. Model simulations were performed with both the CB-IV and CB05 mechanisms for January and July of 2001, representing winter and summer conditions, respectively.

b. Gas-phase chemistry

The CB05 mechanism contains 52 chemical species as shown in Table 1. Additional species in the mechanism include ethane, internal olefins, terpenes, acetaldehyde, higher aldehydes (C_3+ species), formic acid, acetic acid, methanol, ethanol, peroxyacetic acid, higher alkyl peroxy acetyl nitrate analogs, methylhydroperoxide, methylperoxy radical, higher peroxy acyl radical (C_3+ species), and higher (C_2+) organic peroxides. Details of the chemical mechanism are described by Yarwood et al. (2005); only a brief summary is presented here. The major changes in the CB05 mechanism relative to the CB-IV mechanism (Gery et al. 1989) fall into the following categories: kinetic updates, photolysis updates, extended inorganic reaction set, and better representation of atmospheric chemistry of ethane, higher aldehydes, alkenes with internal double bonds, oxygenated products and intermediates, and terpenes.

Kinetic data for the rate constant expressions were updated from the most recent evaluations by the International Union of Pure and Applied Chemistry (IUPAC) (Atkinson et al. 2005) and National Aeronautics and Space Administration/Jet Propulsion Laboratory (Sander et al. 2003) review panels. Photolysis data for the CB05 mechanism have been taken from the IUPAC evaluation (Atkinson et al. 2005) and the SAPRC-99 mechanism (Carter 2000).

TABLE 1. Species names for the CB05 mechanism. The * symbol indicates a new species in the CB05 mechanism.

Species name	Description	Species name	Description
NO	Nitric oxide	MEO2	Methylperoxy radical*
NO2	Nitrogen dioxide	MEOH	Methanol*
O3	Ozone	MEPX	Methylhydroperoxide*
O	Oxygen atom (triplet)	FACD	Formic acid*
O1D	Oxygen atom (singlet)	ETHA	Ethane*
OH	Hydroxyl radical	ROOH	Higher organic peroxide*
HO2	Hydroperoxy radical	AACD	Higher carboxylic acid*
H2O2	Hydrogen peroxide	PACD	Higher peroxycarboxylic acid*
NO3	Nitrate radical	PAR	Paraffin carbon bond
N2O5	Dinitrogen pentoxide	ROR	Secondary alkoxy radical
HONO	Nitrous acid	ETH	Ethene
HNO3	Nitric acid	OLE	Terminal olefin carbon bond
PNA	Peroxynitric acid	IOLE	Internal olefin carbon bond*
CO	Carbon monoxide	ISOP	Isoprene
FORM	Formaldehyde	ISPD	Isoprene product
ALD2	Acetaldehyde*	TERP	Terpene*
C2O3	Acetylperoxy radical	TOL	Toluene and other monoalkyl aromatics
PAN	Peroxyacetyl nitrate	XYL	Xylene and other polyalkyl aromatics
ALDX	Higher aldehyde*	CRES	Cresol and higher MW weight phenols
CXO3	Higher acylperoxy radical*	TO2	Toluene-hydroxyl radical adduct
PANX	Higher peroxyacyl nitrate*	OPEN	Aromatic ring opening product
XO2	NO to NO2 conversion (from RO2)	CRO	Methylphenoxy radical
XO2N	NO to RNO3 conversion (from RO2)	MGLY	Methylglyoxal and related products
NTR	Organic nitrate (RNO3)	SO2	Sulfur dioxide
ETOH	Ethanol*	SULF	Sulfuric acid (gaseous)
CH4	Methane	HCO3	Adduct formed from FORM and HO2*

Several nitrogen oxides (NO_x) recycling reactions have been added to the CB05 mechanism to improve the representation of the fate of NO_x over multiday time scales (Zaveri and Peters 1999). An explicit reaction between hydroxyl radical (OH) and ethane (ETHA) was added to better describe the chemistry of remote atmospheres. A new higher aldehyde species (ALDX) was added.

A new species (internal olefins) was added to represent alkenes with internal double bonds such as 2-butenes. Internal olefins (IOLE) were previously represented by their aldehyde products in the CB-IV mechanism. Including IOLE explicitly in the CB05 mechanism better describes the kinetics of internal olefins than the CB-IV mechanism approach. The IOLE chemistry is improved by having both acetaldehyde (ALD2) and lumped higher aldehydes (ALDX) as reaction products. A new species TERP and its related reactions, based on the SAPRC-99 chemistry (Carter 2000), were added in the CB05 mechanism to represent terpenes. Reactions of methanol (MEOH) and ethanol (ETOH) were also added.

The CB05 mechanism has been evaluated by comparing simulation results with data from the University of North Carolina, Chapel Hill, and the University of California, Riverside. Yarwood et al. (2005) performed simulations using the CB05 mechanism and compared the results with the chamber experimental data. In general, the CB05 mechanism performed as well as or in some cases better than the CB-IV mechanism in simulating the data.

c. Aerosol chemistry

A brief discussion on aerosol chemistry is provided here; a detailed description can be found elsewhere (Binkowski and Roselle 2003; Byun and Schere 2006). In CMAQ, a modal approach using three lognormal modes is used to describe the aerosol size distribution: Aitken mode, accumulation mode, and coarse mode. Aerosol species that are solved in CMAQ include sulfate, nitrate, ammonium, anthropogenic secondary organic aerosol, anthropogenic primary organic aerosol, biogenic secondary organic aerosol, elemental carbon, sodium chloride, and other unspeciated material. The model accounts for coagulation by Brownian motion and new particle formation by binary homogeneous nucleation of sulfuric acid and water vapor.

The model treats cloud processing of aerosol. Aerosol sulfate production in aqueous phase occurs via oxidation of sulfur by H_2O_2, O_3, oxygen (O_2) catalyzed by manganese (Mn^{2+}) and iron (Fe^{3+}), methylhydroperoxide (MEPX), and peroxycarboxylic acid (PACD).

Aerosol sulfate production in gas phase occurs via reaction between OH and SO_2. The CMAQ also accounts for the treatment of primary sulfate emissions. Gas-phase nitric acid (HNO_3) is produced via homogeneous and heterogeneous reactions which can then partition to form aerosol nitrate. An inorganic aerosol thermodynamic equilibrium model, "ISORROPIA" (version 1.5), is used to determine partitioning of inorganic aerosols in the model (Nenes et al. 1999). Aerosol species in each mode can be removed via dry and wet deposition.

The treatment of secondary organic aerosol (SOA) is also included in the model. Gas-phase chemical reactions of toluene (TOL), xylene (XYL), and cresol (CRES) with OH, and CRES with NO_3 produce semivolatile organic compounds that can condense to form athropogenic SOA. Gas-phase chemical reactions of TERP with OH, O_3, NO_3, and O produce semivolatile organic compounds that can condense to form biogenic SOA. CMAQ allows semivolatile organics compounds in particle phase to evaporate back into gas phase.

TABLE 2. Slope of the linear curve obtained by regression analysis of the results with the CB05 and CB-IV mechanisms (surface layer). CB-IV is the independent variable (X) and CB05 is the dependent variable (Y) in the regression.

Species	Summer	Winter
O_3 (daily max)	1.080	1.008
O_3 (8-h max)	1.083	1.008
NO	0.883	0.970
NO_2	0.987	0.988
FORM	0.879	0.748
H_2O_2	0.532	0.681
OH	0.820	0.992
HO_2	0.740	0.780
N_2O_5	0.676	0.911
HNO_3	0.931	1.008
C_2O_3	0.332	0.247
NO_3	0.738	0.973
ROR	0.767	0.971
CRO	0.127	0.611
Aerosol sulfate (daily avg)	0.916	0.999
Aerosol nitrate (daily avg)	0.980	1.015
Organic carbon (daily avg)	0.902	1.023

d. Emissions

An integral part of any chemical mechanism is the assignment of real organic species to the mechanism species. The existing mapping of the chemical species for the CB-IV mechanism was updated for the CB05 mechanism. The changes were 1) ethane is mapped to ETHA; 2) acetaldehyde is mapped to ALD2; 3) several compounds that produce or react like acetaldehyde are mapped to ALD2; 4) all remaining ALD2 assignments are changed to ALDX; 5) all assignments to 2*ALD2 representing internal olefins are changed to IOLE (internal olefins that are branched at the double bond are represented as aldehyde + PAR because their dominant reaction products are less reactive than the IOLE); and 6) terpenes are mapped to TERP.

The Sparse Matrix Operator Kernel Emission (SMOKE; Houyoux et al. 2000) modeling system (version 2.1) was used to process the 1999 National Emissions Inventory (version 3) to generate model-ready emissions for the CB-IV and CB05 mechanisms. Model-ready emissions files contained emissions of NO, NO_2, SO_2, CO, ammonia, volatile organic compounds, and particulate matter. Biogenic emissions were generated using the Biogenic Emissions Inventory System (Guenther et al. 2000).

3. Results and discussion

a. Comparisons of the predictions from the two mechanisms for summer

To provide an overall assessment of the changes in predicted concentrations with the CB05 mechanism relative to the CB-IV mechanism, a regression analysis was performed to fit a linear curve using results obtained with the two mechanisms. The slopes of these curves for selected species are shown in Table 2. The slope of the curve for daily maximum 1-h O_3 was 1.08, which suggests that the O_3 concentrations predicted using the CB05 mechanism were 8% greater than those predicted by the CB-IV mechanism. A comparison of the daily maximum 1-h O_3 concentrations between the two mechanisms is presented in Fig. 1a. As an example, the domainwide average production and consumption rates of O_3 with the two mechanisms are shown in Table 3 for 1 July. The total O_3 production and the consumption rates were greater with the CB05 mechanism which resulted in a net increased O_3 production; thus the concentrations of O_3 were greater.

The production rate of O_3 via reaction 1 was greater with the CB05 mechanism. The use of quantum yield and absorption cross section data from the SAPRC-99 mechanism into the CB05 mechanism enhanced the photolysis rate of NO_2, which in turn produced more O. The higher O in combination with a higher rate constant increased the production of O_3 via reaction 1 with the CB05 mechanism.

The consumption of O_3 via reaction 2 with the CB05 mechanism was greater than that with the CB-IV mechanism partly because of a higher rate constant. The conversion of NO into NO_2 via $NO + RO_2 \rightarrow RO + NO_2$ with the CB05 mechanism was greater (15%) than that with the CB-IV mechanism (RO_2 = organic peroxy radical and RO = alkoxy radical). Con-

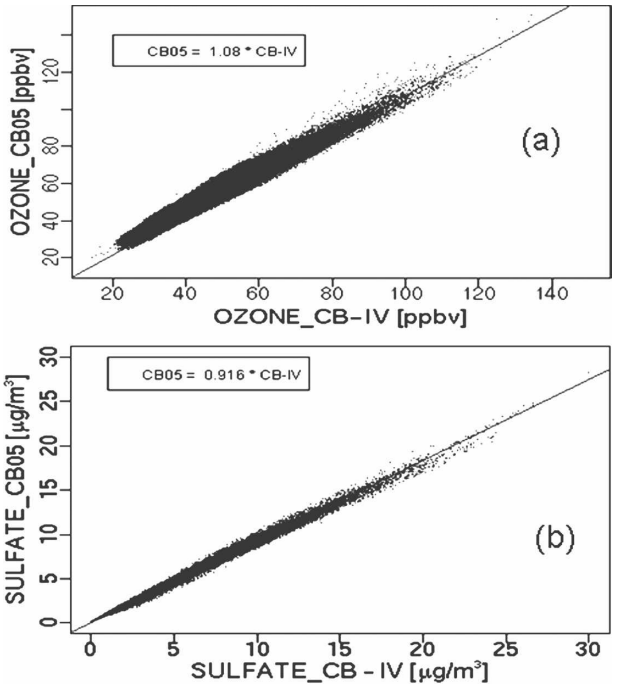

FIG. 1. Comparison of model predictions between the CB-IV and CB05 mechanisms for summer (a) daily maximum 1-h O_3 and (b) aerosol sulfate.

sequently, a lesser amount of NO was available for the titration of O_3 via reaction 2 with the CB05 mechanism than with the CB-IV mechanism. The inclusion of MEO_2 and related chemical reactions in the CB05 mechanism enhanced the conversion of NO into NO_2.

The concentrations of formaldehyde (FORM) with the CB05 mechanism were lower by 12% relative to those with the CB-IV mechanism. As an example, the domainwide average production and consumption rates of FORM with the two mechanisms are shown in Table 4 for 1 July. Total production and consumption rates of FORM with the CB05 mechanism were lower than with the CB-IV mechanism. Reactions 15-b and 16-b produced 22% of the total production of FORM with the CB-IV mechanism, while reactions 15-a and 16-a produced only 2% of the total production of FORM with the CB05 mechanism. The decreased production of FORM via reactions 15-a and 16-a with the CB05 mechanism resulted in a lower total production rate of FORM. The consumption of FORM via each reaction with the CB05 mechanism was lower; thus the total consumption of FORM with the CB05 mechanism decreased relative to that with the CB-IV mechanism. The concentration of FORM was lower with the CB05 mechanism because the net production rate was smaller.

The concentrations of H_2O_2 with the CB05 mechanism were lower than those with the CB-IV mechanism by 47%. The production as well as the consumption rate of H_2O_2 with the CB05 mechanism decreased relative to that with the CB-IV mechanism. The production of H_2O_2 via $HO_2 + HO_2 \rightarrow H_2O_2$ and $HO_2 + HO_2 + H_2O \rightarrow H_2O_2$ decreased with the CB05 mechanism because of lower rate constants and lower HO_2 concentrations. The consumption of H_2O_2 via $H_2O_2 \rightarrow 2^*OH$ and $H_2O_2 + OH \rightarrow HO_2$ also decreased with the CB05 mechanism. The CB05 mechanism includes two additional reactions involving H_2O_2 (OH + OH →

TABLE 3. Domainwide average production and consumption rates of O_3 with the CB-IV and CB05 mechanisms on 1 Jul (surface layer). An average value for each grid cell was first calculated using data from 1400 to 2200 UTC. A domainwide average was then calculated using all gridcell average values in the modeling domain. The CB05 mechanism has additional reactions related to O_3 ($C_2O_3 + HO_2 = 0.2O_3$; $C_xO_3 + HO_2 = 0.2O_3$; $NO_3 + O_3 = NO_2$). The production and consumption rates of O_3 from these reactions were relatively small and are omitted to conserve space. Consumption rates of O_3 via reactions with all organic species are combined into VOC + O_3. To conserve space, most reaction products have been omitted.

		CB05 mechanism	CB-IV mechanism
No.	Reaction producing O_3	Production rate (ppbv min^{-1})	Production rate (ppbv min^{-1})
1	$O + O_2 + M \rightarrow O_3$	1.023	0.905
	Total production rate	1.023	0.905
	Reactions consuming O_3	Consumption rate (ppbv min^{-1})	Consumption rate (ppbv min^{-1})
2	$NO + O_3 \rightarrow$	0.106	0.0952
3	$NO_2 + O_3 \rightarrow$	8.02×10^{-4}	7.42×10^{-4}
4	$O_3 \rightarrow$	0.842	0.746
5	$O_3 \rightarrow$	5.87×10^{-2}	4.82×10^{-2}
6	$O_3 + OH \rightarrow$	8.03×10^{-4}	8.13×10^{-4}
7	$HO_2 + O_3 \rightarrow$	2.01×10^{-3}	2.41×10^{-3}
8	VOC + $O_3 \rightarrow$	1.27×10^{-3}	5.86×10^{-4}
	Total consumption rate	1.01	0.893
	Net production rate	0.012	0.011

TABLE 4. Domainwide average production and consumption rates of FORM with the CB-IV and CB05 mechanisms on 1 Jul (surface layer). Domain average values are calculated using similar procedure as for the values in Table 3, except that data from all 24 h were used. The productions of FORM from MEPX in the CB05 mechanism and from $C_2O_3 + C_2O_3$ in the CB-IV mechanism were small and are omitted. The CB05 mechanism also includes two additional reactions ($FORM + HO_2 = HCO_3$ and $HCO_3 = FORM + HO_2$). The net production of FORM from these reactions was $\sim 10^{-8}$ ppbv min^{-1}; these reactions are omitted.

	CB05			CB-IV	
No.	Reactions producing FORM	Production rate (ppbv min^{-1})	No.	Reactions producing FORM	Production rate (ppbv min^{-1})
9-a	VOC + O →	1.48×10^{-6}	9-b	VOC + O →	1.37×10^{-6}
10-a	VOC + OH →	2.70×10^{-3}	10-b	VOC + OH →	2.93×10^{-3}
11-a	VOC + O_3 →	6.72×10^{-4}	11-b	VOC + O_3 →	4.79×10^{-4}
12-a	VOC + NO_3 →	8.99×10^{-7}	12-b	VOC + NO_3 →	2.87×10^{-5}
13-a	MEO_2 + NO →	1.91×10^{-3}	13-b	CH_4 + OH →	1.75×10^{-3}
14-a	$MEO_2 + MEO_2$ →	1.04×10^{-4}			
15-a	$C_2O_3 + MEO_2$ →	1.22×10^{-4}	15-b	C_2O_3 + NO →	1.28×10^{-3}
16-a	$CxO_3 + MEO_2$ →	7.19×10^{-6}	16-b	$C_2O_3 + HO_2$ →	2.15×10^{-4}
	Total production rate	5.58×10^{-3}		Total production rate	6.72×10^{-3}
	Reactions consuming FORM	Consumption rate (ppbv min^{-1})		Reactions consuming FORM	Consumption rate (ppbv min^{-1})
18-a	FORM + OH →	8.81×10^{-4}	18-b	FORM + OH →	1.48×10^{-3}
19-a	FORM →	4.75×10^{-4}	19-b	FORM →	5.40×10^{-4}
20-a	FORM →	6.92×10^{-4}	20-b	FORM →	7.06×10^{-4}
21-a	FORM + O →	2.98×10^{-8}	21-b	FORM + O →	3.82×10^{-8}
22-a	FORM + NO_3 →	1.71×10^{-6}	22-b	FORM + NO_3 →	3.23×10^{-6}
	Total consumption rate	2.05×10^{-3}		Total consumption rate	2.72×10^{-3}
	Net production rate	3.53×10^{-3}		Net production rate	4.00×10^{-3}

H_2O_2 and $H_2O_2 + O \rightarrow OH + HO_2$). However, these reactions did not affect the net production rate since their contributions were small. The net production rate decreased with the CB05 mechanism primarily because of lower production of H_2O_2 via $HO_2 + HO_2 \rightarrow H_2O_2$ and $HO_2 + HO_2 + H_2O \rightarrow H_2O_2$.

As shown in Fig. 1b and Table 2, the aerosol sulfate concentrations with the CB05 mechanism decreased by 8% relative to those with the CB-IV mechanism. The contribution of emissions and the initial and boundary conditions to aerosol sulfate did not change between the two mechanisms. The production of aerosol sulfate via the gas-phase pathway with the CB05 mechanism was 10% lower than that with the CB-IV mechanism because of lower OH concentration. The production of aerosol sulfate via aqueous-phase pathways with the CB05 mechanism was also lower relative to the CB-IV mechanism. The domainwide aerosol sulfate produced via five aqueous-phase reaction pathways with the two mechanisms is shown in Fig. 2. The reaction of SO_2 with H_2O_2 produced 18% lower aerosol sulfate with the CB05 mechanism because of lower H_2O_2 concentration.

The concentrations of HNO_3 with the CB05 mechanism decreased by 7% relative to those with the CB-IV mechanism. As mentioned in section 2c, the production of HNO_3 in CMAQ occurs via several gas-phase reactions and a heterogeneous reaction between N_2O_5 and water vapor (H_2O). The heterogeneous reaction in CMAQ is implemented in the aerosol module and was used for each mechanism. Thus, the changes in the production of HNO_3 via the heterogeneous reaction depended only on the concentrations of N_2O_5 produced with each mechanism. The production of HNO_3 via the heterogeneous reaction decreased with the CB05 mechanism because of lower N_2O_5 concentrations. The concentrations of N_2O_5 with the CB05 mechanism were lower than those with the CB-IV mechanism by 32% because of the decreased production via $NO_3 + NO_2 \rightarrow N_2O_5$ at night.

The gas-phase production and consumption rates of HNO_3 with the CB05 mechanism were greater than those with the CB-IV mechanism. The additional production of HNO_3 via reactions of $NO_3 + HO_2$, ALDX + NO_3, and NTR + OH with the CB05 mechanism enhanced the total gas-phase production rate of HNO_3. The total gas-phase consumption of HNO_3 increased because of the inclusion of the photolysis of HNO_3 in the CB05 mechanism. The net production of HNO_3 via gas-phase reactions with the CB05 mechanism was slightly greater than with the CB-IV mechanism. The decreases in HNO_3 production via the heterogeneous reaction more than compensated for the increases in HNO_3 production via the gas-phase reac-

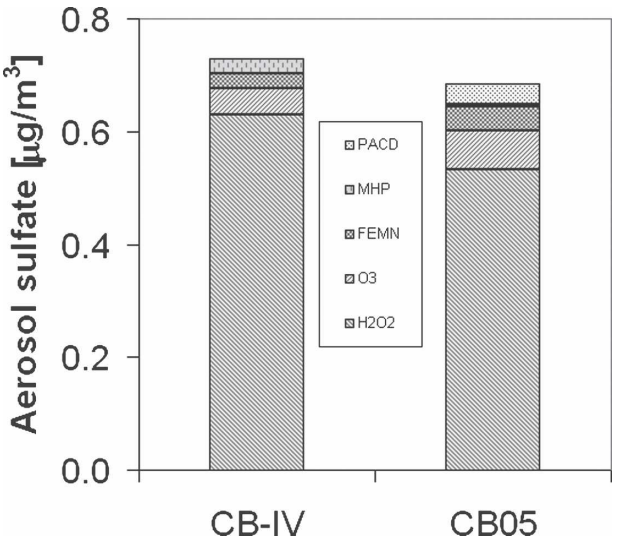

FIG. 2. Comparison of domainwide average aerosol sulfate production via aqueous-phase reaction pathways with the CB-IV and CB05 mechanisms in summer.

tions. Thus, concentrations of HNO_3 were lower with the CB05 mechanism, which led to a decrease in aerosol nitrate concentrations by 2%.

The concentrations of organic carbon (OC) with the CB05 mechanism were 10% lower than those with the CB-IV mechanism. The production of anthropogenic as well as biogenic SOA decreased with the CB05 mechanism; thus the total SOA formation with the CB05 mechanism was lower than with the CB-IV mechanism. It should be noted that only biogenic sources contributed to the emissions of terpenes in the CB-IV mechanism; anthropogenic sources were not accounted for the emissions of terpenes in the CB-IV mechanism. Anthropogenic as well as biogenic sources contributed to the emissions of terpenes in the CB05 mechanism. The contribution of anthropogenic sources to the emissions of terpenes in the CB05 mechanism was only about 1% of the total emissions of terpenes in the modeling domain. Aerosol constituent mass represents the summation of the constituent in the Aitken and accumulation modes. OC further represents the summation of anthropogenic SOA, anthropogenic primary organic aerosol, and biogenic SOA.

b. *Comparisons of the predictions from the two mechanisms for winter*

The predicted concentrations of daily maximum 1- and 8-h O_3 with the CB05 mechanism were within 1% of those with the CB-IV mechanism for winter (Table 2). The predicted concentrations of FORM and H_2O_2 with the CB05 mechanism were lower by 25% and 32%, respectively, relative to those with the CB-IV mechanism. These percent reductions appear to be relatively large; they arise because wintertime concentrations of FORM and H_2O_2 are typically low. The maximum decrease in the absolute concentrations for both species was typically less than 1.0 part per billion by volume (ppbv). The concentrations of aerosol sulfate and nitrate with the CB05 mechanism were within 1% of those with the CB-IV mechanism.

The concentrations of OC with the CB05 mechanism were 2% higher than those with the CB-IV mechanism. The production of anthropogenic SOA increased while the production of biogenic SOA decreased with the CB05 mechanism; thus the total SOA formation with the CB05 mechanism increased.

c. *Spatial variation of the predictions of the two mechanisms*

The differences in the monthly mean concentrations of daily maximum 1-h O_3 between the two mechanisms in summer are shown in Fig. 3a. The largest increases in daily maximum 1-h O_3 concentrations with the CB05 mechanism occurred in northern Texas and western Oklahoma where its concentrations were higher by about 10 ppbv. Large increases (5.0–9.5 ppbv) in O_3 concentrations with the CB05 mechanism also occurred over the central United States. Similar increases were also observed in Southern California, Lake Michigan, Lake Erie, coastal areas of southern and eastern states, and Mexico. Increases in O_3 concentrations with the CB05 mechanism in the remaining areas in the modeling domain ranged between 0 to 5 ppbv. Ozone concentrations with the CB05 mechanism decreased in some areas of Oregon and Washington; however, these decreases were less than 1 ppbv. The spatial distribution of the differences in monthly mean concentrations of daily maximum 8-h O_3 between the two mechanisms was similar to that of the daily maximum 1-h O_3 concentrations. In winter, the largest increases in daily maximum 1- and 8-h O_3 concentrations with the CB05 mechanism were only about 2.0 ppbv and occurred in a grid cell in Mexico. Increases in concentrations of daily maximum 1- and 8-h O_3 over the eastern United States ranged between 1.0 and 1.5 ppbv. Increases in concentrations of daily maximum 1- and 8-h O_3 in the remaining areas of the modeling domain were limited to about 0.5 ppbv.

The changes in the monthly mean concentrations of FORM with the CB05 mechanism relative to those with the CB-IV mechanism in summer are shown in Fig. 3b. While some decreases were observed over most of the United States, the largest decreases occurred in the border areas of Texas, Louisiana, and Arkansas where

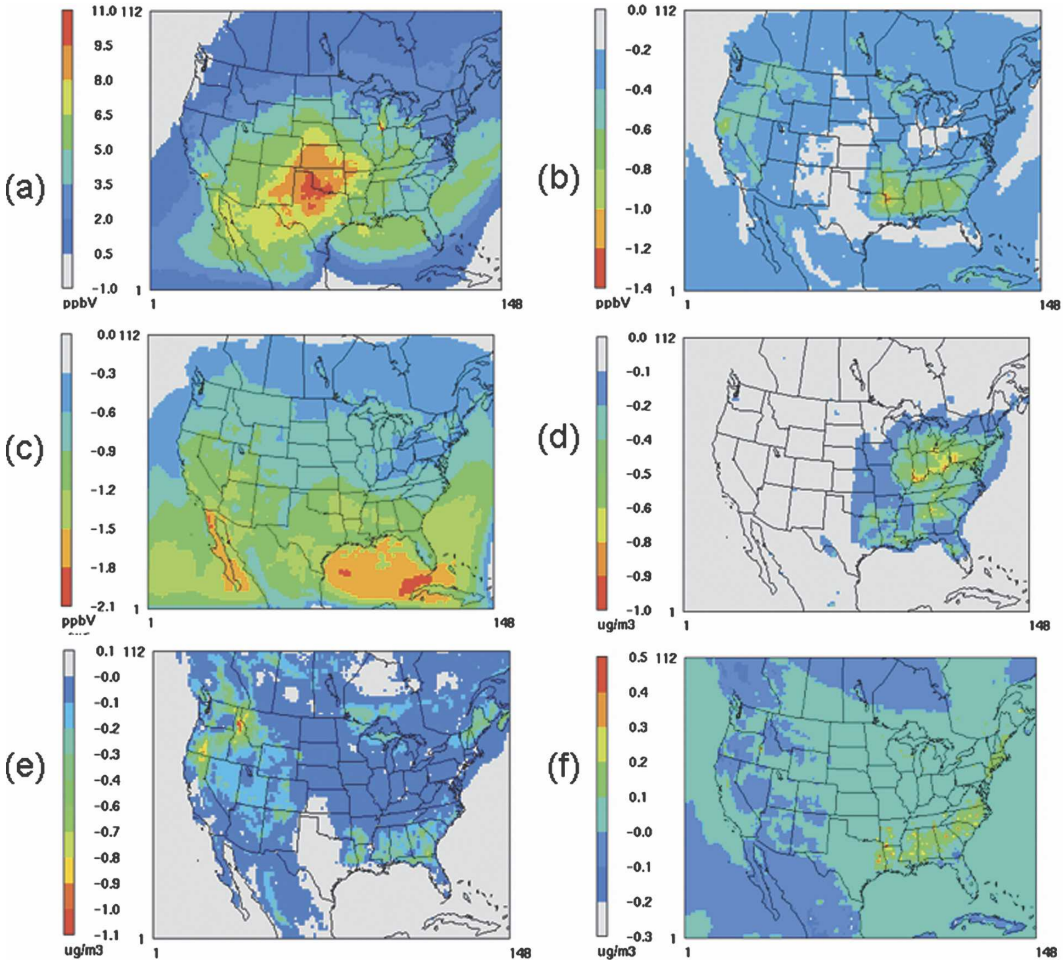

FIG. 3. Changes in monthly mean concentrations between the CB-IV and CB05 (CB05 − CB-IV) mechanisms: (a) daily maximum 1-h O_3 for summer, (b) FORM for summer, (c) H_2O_2 for summer, (d) aerosol sulfate for summer, (e) OC for summer, and (f) OC for winter.

its concentrations were lowered by about 1.1 ppbv. Concentrations of FORM with the CB05 mechanism decreased over parts of Texas, Louisiana, Mississippi, Alabama, Georgia, Arkansas, and Oklahoma by up to 1.0 ppbv. Similar reductions were also observed in parts of California and Idaho. Decreases in the remaining areas were less than 0.6 ppbv. In winter, concentrations of FORM with the CB05 mechanism decreased over the entire modeling domain relative to those with the CB-IV mechanism. Decreases ranging up to 0.4 ppbv occurred over the southern part of the modeling domain. Decreases over the northern part of the modeling domain were small and ranged only up to 0.1 ppbv.

The decreases in the monthly mean concentrations of H_2O_2 with the CB05 mechanism relative to those with the CB-IV mechanism in summer are shown in Fig. 3c. The decreases occurred over most of the modeling domain. The largest decreases occurred in Mexico and the Gulf of Mexico where its concentrations were lowered by more than 1.8 ppbv. Decreases in the southern part of the modeling domain generally ranged between 0.9 to 1.8 ppbv, and decreases in the northern part of the modeling domain were less than 0.9 ppbv. In winter, concentrations of H_2O_2 with the CB05 mechanism also decreased over the entire modeling domain relative to those with the CB-IV mechanism. However, these decreases were smaller relative to those in summer. Decreases ranging up to 0.7 ppbv occurred over the southern part of the modeling domain. Decreases over the northern part of the modeling domain were small and ranged only up to 0.1 ppbv.

The decreases in the monthly mean concentrations of aerosol sulfate with the CB05 mechanism relative to those with the CB-IV mechanism in summer are shown in Fig. 3d. The decreases were mostly limited to the eastern United States. The largest decreases occurred

in Indiana, Ohio, Pennsylvania, and Georgia where its concentrations were lowered by more than 0.9 $\mu g\ m^{-3}$. Concentrations of aerosol sulfate with the CB05 mechanism decreased in the Ohio Valley, Alabama, Georgia, Florida, Louisiana, North Carolina, Tennessee, and the border area of Texas, Oklahoma, and Arkansas by up to 0.9 $\mu g\ m^{-3}$. The decreases in the remaining areas of the eastern United States were less than 0.4 $\mu g\ m^{-3}$.

The changes in the monthly mean concentrations of OC with the CB05 mechanism relative to those with the CB-IV mechanism in summer are shown in Fig. 3e. The decreases in the concentrations of OC with the CB05 mechanism occurred mostly in the western United States, the Southeast, Vermont, Maine, and New Hampshire. The largest decreases occurred in Idaho where its concentrations were lowered by up to 1.1 $\mu g\ m^{-3}$. Decreases in other parts of the western U.S. ranged up to 1.0 $\mu g\ m^{-3}$. Decreases in the Southeast ranged up to 0.7 $\mu g\ m^{-3}$, while the decreases in Maine, Vermont, and New Hampshire ranged up to 0.4 $\mu g\ m^{-3}$. The concentrations of OC with the CB05 mechanism increased in a few grid cells across the modeling domain in summer; however, these increases were less than 0.1 $\mu g\ m^{-3}$. The changes in concentrations of OC between the two mechanisms in winter are shown in Fig. 3f. Concentrations of OC increased in parts of the Southeast, parts of the Northeast, California, Oregon, Washington, Idaho, and Mexico by up to 0.5 $\mu g\ m^{-3}$. Concentrations of OC decreased in parts of Georgia, Florida, the western United States, Canada, and Mexico by up to 0.3 $\mu g\ m^{-3}$.

d. Comparison of the model predictions with observed data

Ambient monitoring data from three monitoring networks are used to compare the model predictions for aerosol: Interagency Monitoring of Protected Visual Environments (IMPROVE), Clean Air Status and Trends Network (CASTNet), and Speciation Trends Network (STN). Ambient monitoring data from the EPA's Air Quality System (AQS) and CASTNet are used to compare the model performance for O_3 concentrations. Various statistical measures can be used to evaluate model performance; the following measures were chosen for this study: normalized mean bias (NMB), normalized mean error (NME), and root-mean-square error (RMSE; Eder and Yu 2006). Since the CMAQ predictions with the CB05 mechanism were closer to those with the CB-IV mechanism during winter, model predictions are compared with observed data only for summer.

Performance statistics of the concentrations of daily maximum 1- and 8-h O_3 obtained with the two mechanisms in urban and rural areas are presented in Table 5. Data from the AQS sites are used to evaluate model performance in urban areas. In urban areas, the predicted mean concentration of daily maximum 1-h O_3 with the CB-IV mechanism was slightly lower than the observed mean, while the predicted mean concentration with the CB05 mechanism was greater than the observed mean. The concentration of daily maximum 1-h O_3 with the CB-IV mechanism was biased slightly negative and the concentration with the CB05 mechanism was biased positive. The NMB for the concentrations of daily maximum 1-h O_3 with the CB05 mechanism deteriorated slightly relative to those with the CB-IV mechanism. The NME and RMSE with the CB05 mechanism, however, did not change substantially relative to those with the CB-IV mechanism. While the model bias for O_3 in urban areas deteriorated slightly relative to that with the CB-IV mechanism, the model bias with the CB05 mechanism actually improved at higher observed concentrations (Appel et al. 2007). The model tends to overpredict O_3 at lower observed concentrations with both mechanisms partly because of the use of a reduced number of vertical layers and clean-air vertical profiles. The model overpredictions at lower observed concentrations can be improved by using additional vertical layers and results from global air quality models as boundary conditions (Appel et al. 2007). The mean concentrations of daily maximum 8-h O_3 with both mechanisms were higher than the observed mean. The NMB with the CB05 mechanism in urban

TABLE 5. Performance statistics for O_3 in urban and rural areas during summer.

Urban area (data from AQS sites)				
	1-h max		8-h max	
Metric	CB05	CB-IV	CB05	CB-IV
No.	34 266	34 266	34 241	34 241
Mean modeled (ppbv)	62.1	58.0	57.4	53.3
Mean observed (ppbv)	58.6	58.6	51.1	51.1
NMB (%)	6.1	−0.86	12.4	4.3
NME (%)	19.5	19.1	21.8	19.9
RMSE (ppb)	14.9	14.8	14.1	13.0
Rural area (data from CASTNet sites)				
	1-h max		8-h max	
Metric	CB05	CB-IV	CB05	CB-IV
No.	2 250	2 250	2 248	2 248
Mean modeled (ppbv)	54.7	54.2	51.8	51.3
Mean observed (ppbv)	56.2	56.2	50.9	50.9
NMB (%)	3.1	−3.7	8.1	0.8
NME (%)	15.9	16.7	17.7	17.1
RMSE (ppb)	11.4	12.0	11.2	11.0

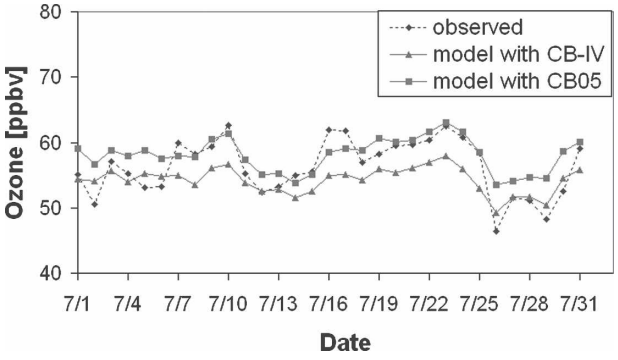

FIG. 4. Comparison of predicted daily maximum 1-h O_3 with observed data during summer in rural areas.

areas deteriorated slightly relative to that with the CB-IV mechanism while the NME and RMSE did not change considerably.

Data from the CASTNet sites were used to evaluate model performance in rural areas. As shown in Table 5, the predicted mean concentrations of daily maximum 1-h O_3 with both mechanisms were lower than the observed mean for rural areas. However, the mean concentration with the CB05 mechanism was closer to the observed data than that of the CB-IV mechanism. The NMB for concentrations of the daily maximum 1-h O_3 with the CB05 mechanism improved slightly relative to those with the CB-IV mechanism. The NME and RMSE with the CB05 mechanism, however, did not change substantially relative to those with the CB-IV mechanism. The mean concentration of daily maximum 8-h O_3 with each mechanism was slightly greater than the observed data. The NMB with the CB05 mechanism deteriorated slightly relative to that with the CB-IV mechanism while the NME and RMSE did not change considerably.

Average concentrations of daily maximum 1-h O_3 with the CB-IV and CB05 mechanisms are compared with the mean observed data for rural areas in Fig. 4. Predicted concentrations with the CB-IV mechanism agrees better with the observed data on 1–6, 12–13, and 26–30 July. However, concentrations with the CB05 mechanism are in better agreement with the observed data on remaining days in the month. Predicted concentrations with the CB05 mechanism capture the day-to-day variability in the observed data better than those with the CB-IV mechanism.

Predicted vertical O_3 concentrations with the CB-IV and CB05 mechanisms are compared with ozonesonde data at three stations in Fig. 5: Wallops Island, Virginia; Boulder, Colorado; and Huntsville, Alabama. Weekly ozonesonde measurements are available for these stations (http://www.woudc.org/data_e.html). Averages of all available data for each site are shown in Fig. 5. For

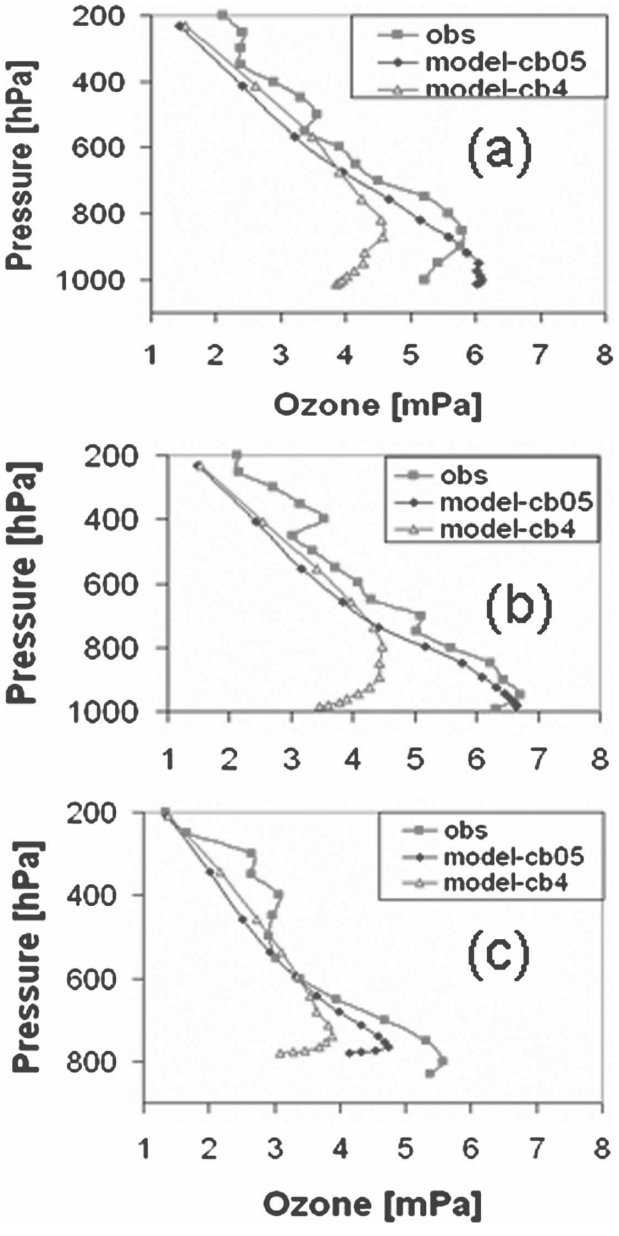

FIG. 5. Comparison of predicted vertical O_3 with ozonesonde data from (a) Wallops Island, (b) Huntsville, and (c) Boulder, for summer.

all three stations, predicted O_3 concentrations with the CB05 mechanism had better agreements with the ozonesonde data than those predicted with the CB-IV mechanism from surface level up to a height of about 700 hPa. While the CB-IV mechanism performed slightly better than the CB05 mechanism above 700 hPa, the differences between the two mechanisms were small. Thus, the model performance with the CB05 mechanism at high altitudes improved relative to the CB-IV mechanism.

Performance statistics of the observed and predicted

TABLE 6. Performance statistics for aerosol sulfate and organic carbon during summer.

Species	Metric	IMPROVE		CASTNet		STN	
		CB05	CB-IV	CB05	CB-IV	CB05	CB-IV
Aerosol sulfate	No.	1108	1108	291	291	698	698
	Mean modeled	1.7	1.8	3.1	3.3	3.5	3.8
	Mean observed	2.4	2.4	4.4	4.4	4.4	4.4
	NMB (%)	−30.9	−25.8	−30.1	−24.1	−21.7	−15.3
	NME (%)	43.9	42.3	33.2	29.0	37.2	35.7
	RMSE (μg m^{-3})	1.9	1.8	2.2	2.0	2.5	2.4
Organic carbon	No.	1117	1117				
	Mean modeled	1.22	1.37				
	Mean observed	1.20	1.20				
	NMB (%)	1.8	14.6				
	NME (%)	66.8	72.4				
	RMSE (μg m^{-3})	1.10	1.19				

aerosol sulfate concentrations with the two mechanisms are shown in Table 6. The NMB for aerosol sulfate with the CB05 mechanism deteriorated slightly for all monitoring networks relative to those with the CB-IV mechanism. However, the NME and RMSE with the CB05 mechanism for aerosol sulfate did not change considerably relative to those with the CB-IV mechanism. The slight deterioration of the NMB for aerosol sulfate with the CB05 mechanism occurs because of overprediction of the precipitation by the meteorological driver for the CMAQ modeling system (MM5) at 36-km grid spacing. The precipitation overprediction is reduced at 12-km grid spacing. To further evaluate the model performance for aerosol sulfate, two additional model simulations were performed for the eastern United States using 12-km grid spacing. Results of these model simulations indicate that the NMB for aerosol sulfate for STN monitoring network improved slightly from 13.0% with the CB-IV mechanism to 4.4% with the CB05 mechanism in summer. The NME for aerosol sulfate changed from 38.5% with the CB-IV mechanism to 35.0% with the CB05 mechanism.

Performance statistics of the observed and predicted OC concentrations with the two mechanisms are also shown in Table 6. The NMB and NME for OC with the CB05 mechanism improved relative to the CB-IV mechanism.

4. Summary

We have implemented the new CB05 mechanism into the CMAQ modeling system and performed simulations for a winter and summer month of 2001 using the CB-IV and CB05 mechanisms. Differences in predictions obtained with the two mechanisms were small for most species in winter. However, relatively large differences in predicted concentrations were observed for many species in summer.

Model O_3 predictions with the CB05 mechanism improved relative to those with the CB-IV mechanism at high-altitude conditions. Concentrations of daily maximum 1-h O_3 with the CB05 mechanism improved slightly in rural areas. Model OC predictions with the CB05 mechanism improved relative to those with the CB-IV mechanism.

We are currently performing a comprehensive comparison of the model predictions with the CB-IV, CB05, and SAPRC-99 mechanisms including their sensitivities to emissions. As a part of this study, we are also performing additional comparisons of model predictions with observed data with longer and larger datasets to further examine the comparisons described here. Future studies should also focus on the comparison of model predictions with the CB05 mechanism with those with the Regional Atmospheric Chemistry Mechanism (RACM).

Acknowledgments. Charles Chang of Computer Sciences Corporation prepared the model-ready emissions files for the study. The research presented here was performed under the Memorandum of Understanding between the U.S. Environmental Protection Agency and the U.S. Department of Commerce's National Oceanic and Atmospheric Administration (NOAA) and under agreement number DW13921548. This work constitutes a contribution to the NOAA Air Quality Program. Although it has been reviewed by the EPA and NOAA and approved for publication, it does not necessarily reflect their policies or views.

REFERENCES

Adelman, Z. E., 1999: A reevaluation of the Carbon Bond-IV photochemical mechanism. M.S. thesis, Department of Envi-

ronmental Sciences and Engineering, School of Public Health, University of North Carolina, Chapel Hill, 194 pp. [Available online at http://airsite.unc.edu/soft/cb4/FINAL.pdf.]

Appel, K. W., A. B. Gilliland, G. Sarwar, and R. C. Gilliam, 2007: Evaluation of the Community Multiscale Air Quality (CMAQ) model version 4.5: Uncertainties and sensitivities impacting model performance Part I: Ozone. *Atmos. Environ.,* **41,** 9603–9615.

Atkinson, R., and Coauthors, cited 2005: Summary of evaluated kinetic and photochemical data for atmospheric chemistry. [Available online at http://www.iupac-kinetic.ch.cam.ac.uk/summary/IUPACsumm_web_March2005.pdf.]

Binkowski, F. S., and S. J. Roselle, 2003: Models-3 Community Multiscale Air Quality (CMAQ) model aerosol component 1. Model description. *J. Geophys. Res.,* **108,** 4183, doi:10.1029/2001JD001409.

Byun, D., and K. L. Schere, 2006: Review of the governing equations, computational algorithms, and other components of the Models-3 Community Multiscale Air Quality (CMAQ) modeling system. *Appl. Mech. Rev.,* **59,** 51–77.

Carter, W. P. L., cited 2000: Implementation of the SAPRC-99 chemical mechanism into the Models-3 Framework. Report to the United States Environmental Protection Agency. [Available online at http://www.cert.ucr.edu/~carter/absts.htm#s99mod3.]

Dodge, M. C., 2000: Chemical oxidant mechanisms for air quality modeling: Critical review. *Atmos. Environ.,* **34,** 2103–2130.

Eder, B., and S. Yu, 2006: A performance evaluation of the 2004 release of Models-3 CMAQ. *Atmos. Environ.,* **40,** 4811–4824.

Gery, M. W., G. Z. Whitten, J. P. Killus, and M. C. Dodge, 1989: A photochemical kinetics mechanism for urban and regional scale computer modeling. *J. Geophys. Res.,* **94** (D10), 12 925–12 956.

Grell, G., J. Dudhia, and D. Stauffer, 1994: A description of the fifth-generation Penn State/NCAR Mesoscale Model (MM5). NCAR Tech. Note NCAR/TN-398+STR, 122 pp.

Guenther, A., C. Geron, T. Pierce, B. Lamb, P. Harley, and R. Fall, 2000: Natural emissions of non-methane volatile organic compounds, carbon monoxide, and oxides of nitrogen from North America. *Atmos. Environ.,* **34,** 2205–2230.

Houyoux, M. R., J. M. Vukovich, C. J. Coats Jr., N. M. Wheeler, and P. S. Kasibhatla, 2000: Emission inventory development and processing for the Seasonal Model for Regional Air Quality (SMRAQ) project. *J. Geophys. Res.,* **105,** 9079–9090.

Nenes, A., C. Pilinis, and S. N. Pandis, 1999: Continued development and testing of a new thermodynamic aerosol module for urban and regional air quality models. *Atmos. Environ.,* **33,** 1553–1560.

Sander, S. P., and Coauthors, 2003: Chemical kinetics and photochemical data for use in atmospheric studies, evaluation number 14. NASA Jet Propulsion Laboratory. [Available online at http://jpldataeval.jpl.nasa.gov/pdf/JPL_02-25_rev02.pdf.]

Whitten, G. Z., H. Hogo, and J. P. Killus, 1980: The carbon-bond mechanism: A condensed kinetic mechanism for photochemical smog. *Environ. Sci. Technol.,* **14,** 690–700.

Yarwood, G., S. Rao, M. Yocke, and G. Whitten, cited 2005: Updates to the carbon bond chemical mechanism: CB05. Final report to the U.S. EPA, RT-0400675. [Available online at http://www.camx.com.]

Zaveri, R. A., and L. K. Peters, 1999: A new lumped structure photochemical mechanism for large-scale applications. *J. Geophys. Res.,* **104,** 30 387–30 416.